buildings

MDPI

Article

Application of Resistometric Sensors in Investigation of Zinc Corrosion in Simulated Concrete Environments

Matěj Reiser [1,*], Milan Kouřil [1], Pietro Forcellese [2] and Tiziano Bellezze [2]

[1] Department of Metals and Corrosion Engineering, University of Chemistry and Technology in Prague, 160 00 Prague, Czech Republic
[2] Department of Science and Engineering of Matter, Environment and Urban Planning, Marche Polytechnic University, 60121 Ancona, Italy
* Correspondence: reiserm@vscht.cz

Abstract: The aim of this paper was to investigate the corrosion behaviour of zinc in simulated concrete solutions using resistometric sensors and to describe the kinetics of zinc corrosion. The sensors provide corrosion data information in real time; thus, it is a useful technique for observing zinc corrosion behaviour in concrete environments. The replacement of carbon steel rebar by galvanized steel in concrete is a discussable topic with contradictory results in the literature presented in the introduction. In our case, zinc resistometric sensors were used, and they showed results in good agreement with other techniques, such as corrosion potential monitoring and EIS measurements. According to our results, zinc is able to passivate in a simulated concrete solution and even in a simulated carbonated solution. The corrosion rate was reduced by almost 40 times, during the active to passive transition. The zinc remains passive even in simulated concrete solutions contaminated with low levels of chloride ions up to 0.9 wt.%.

Keywords: resistometric sensors; galvanized steel; concrete; corrosion monitoring

check for updates

Academic Editor: Ray Kai Leung Su

Received: 23 January 2025
Revised: 11 February 2025
Accepted: 17 February 2025
Published: 19 February 2025

Citation: Reiser, M.; Kouřil, M.; Forcellese, P.; Bellezze, T. Application of Resistometric Sensors in Investigation of Zinc Corrosion in Simulated Concrete Environments. *Buildings* **2025**, *15*, 635. https://doi.org/10.3390/buildings15040635

1. Introduction

Reinforced concrete is one of the most used materials in the construction industry. Carbon steel, which is commonly used as a reinforcement, becomes passive right after embedding in concrete, and, thus, its corrosion rate is almost negligible. Nevertheless, during its lifetime, reinforced concrete degrades due to factors such as chloride penetration, carbonation, etc. At this moment the corrosion resistance of the reinforcement is crucial. If the reinforcement begins to corrode, the load capacity of the rebars decreases, and most importantly, the formed corrosion products may cause cracks in the concrete due to their volume expansion [1,2]. The presence of cracks in a structure needs to be avoided or at least delayed. There are several methods for doing so, such as the use of more corrosion resistant rebar, the use of inhibitors in concrete, corrosion protection of the rebars by coatings or by electrochemical polarization, electrochemical extraction of chlorides from the concrete and the use of cement with a reduced water–cement ratio [3].

The use of galvanized steel as a reinforcement in concrete instead of carbon steel could prolong the lifetime of reinforced concrete structures. It is believed that the initial cost of galvanized steel would repay itself by prolonging service time and reducing repair costs [4]. Galvanized steel reinforcement, if in a passive state, could last considerably longer. Galvanized steel doesn't become passive right after embedding in fresh concrete, rather it needs a certain amount of time to form a stable passive layer [5]. Meanwhile, zinc corrodes actively while producing hydrogen, which leads to increased porosity of the cement binder at the rebar surface. The zinc surface stabilizes after 30 h in concrete due to the formation of a thick layer of a protective corrosion product—calcium hydroxyzincate (CHZ)—$Ca[Zn(OH)_3]_2 \cdot 2H_2O$ [6,7]. The passivation mechanism is shown in the following Equations (1)–(4) [8].

$$Zn + 4\,OH^- \rightarrow Zn(OH)_4^{2-} + 2\,e^- \tag{1}$$

$$Zn + 2\,OH^- \rightarrow ZnO + 2\,e^- + H_2O \tag{2}$$

$$ZnO + H_2O + 2\,OH^- \rightarrow Zn(OH)_4^{2-} \tag{3}$$

$$2\,Zn(OH)_4^{2-} + Ca^{2+} + 2\,H_2O \rightarrow Ca[Zn(OH)_3]_2 \cdot 2\,H_2O + 2\,OH^- \tag{4}$$

The morphology of the formed CHZ depends on pH: at a pH around 12.6, the surface is completely covered by a compact layer of CHZ; when a passive layer is formed, it is stable up to about pH 13.6; above pH 13.6, the complete passivation of the whole surface is not possible. and only isolated crystals of CHZ remain while the zinc surface corrodes [5]. Calcium hydroxyzincate, if in the appropriate pH zone, can fill the pores and thus lowers porosity which eventually leads to improvement of bond strength [9]. Hydrogen gas formation can be eliminated by artificial passivation of galvanized steel by means of Cr(VI) [5].

Thus, zinc or galvanized steel can be passive in fresh concrete after a certain time, even increasing the bond strength between the rebar and concrete [7,10]. More importantly, the zinc is able to passivate even during carbonation, which carbon steel cannot do. If the carbonation of concrete occurs, calcium hydroxyzincate, formed in the environment of fresh concrete, turns into hydrozincite ($Zn_5(CO_3)_2(OH)_6$) and calcite ($CaCO_3$), as shown in Equation (5).

$$5\,Ca[Zn(OH)_3]_2 \cdot 2\,H_2O + 9\,CO_2 \rightarrow 2\,Zn_5(CO_3)_2(OH)_6 + 5\,CaCO_3 + 19\,H_2O \tag{5}$$

Protective properties of that layer are lower than for calcium hydroxyzincate, according to impedance measurements [7]. In addition, a threshold chloride concentration for galvanized steel activation is higher than for common steel, which means the use of galvanized steel prolongs the lifetime of concrete structures [5,11]. In a concrete contaminated by chlorides, the solid corrosion products of galvanized steel are different and contain chlorides; $Zn_5(OH)_8Cl_2 \cdot H_2O$ and ZnO are found on the galvanized steel surface. $Zn_5(OH)_8Cl_2 \cdot H_2O$ is an undesired corrosion product because of its higher volume expansion, which can eventually lead to concrete cracking [12]. The formation of $Zn_5(OH)_8Cl_2 \cdot H_2O$ is shown in Equation (6).

$$5\,Ca[Zn(OH)_3]_2 \cdot 2\,H_2O + 14\,NaCl \rightarrow 2\,Zn_5(OH)_2Cl_2 \cdot H_2O + 5\,CaCl_2 + 14\,NaOH + 8\,H_2O \tag{6}$$

On the other hand, there are several experimental works published, according to which the use of the galvanized steel as a reinforcement should be taken into consideration. In fact, some authors [12] showed a reduced bonding strength between galvanized steel reinforcement and concrete compared to common carbon steel rebars by means of pull-out tests. They found that the CHZ layer is rough and thus improves adhesion to concrete, but intergranular ruptures that occur decrease the bond strength. In addition, the authors claim that interphase cement binder porosity induced by hydrogen evolution is not completely filled by the CHZ, which results in reduced bond strength of the galvanized steel with concrete. There are other problems related to the use of galvanized steel as a rebar, such as unknown effect of additives in modern concrete mixtures. According to these results, it is important to verify the corrosion resistance of galvanized steel rebars or to better apply an additional surface treatment to galvanized rebars [13,14].

Regarding oxidizing agent availability for the corrosion reaction of zinc, there are water and oxygen to consider in the concrete pore solution. Some studies show that the water is the main oxidant, others claim that it is the oxygen. According to experiments of different concrete specimens in aqueous and dry conditions with or without oxygen availability, the zinc corrosion rate depends mainly on the water's presence. Oxygen plays an important role but water serves as a main depolarization agent in the cathodic corrosion reaction, as was proved by Pokorny et al., which supports the theory that the zinc surface is passive due to not only calcium hydroxyzincate but also due to the presence of ZnO and $Zn(OH)_2$ inside the CHZ pores [15]. From the other point of view, oxygen is the main oxidizing agent necessary for zinc passivation by only calcium hydroxyzincate in a concrete environment. In well aerated environments, i.e., with high oxygen concentration, the more protective CHZ-based passive layer is formed on the surface of galvanized steel [10].

Further research is needed for a better understanding of the contradictory published results regarding the impact of zinc corrosion on the applicability of galvanized steel as a substitute of carbon steel reinforcement in concrete.

In this study, the resistometric technique was chosen to measure the corrosion rate of zinc in a simulated concrete environment. A zinc foil track at the resistometric sensor represented the topmost zinc layer of the galvanized steel in the experiments. The principle of resistometric technique is based on measuring the electrical resistance of the resistometric sensor's metallic tracks. As the metallic track corrodes, the thickness lowers, and the electrical resistance increases. The scheme of the resistometric sensor is shown on Figure 1. It consists of a metallic track divided into two parts—a measurement part and a reference part. The measurement part is in contact with the environment, and the reference part is masked and thus isolated from the environment, the main role of the reference part is to compensate for the impact of temperature variations on the electrical resistance reading. The measurement part (exposed) is allowed to corrode, and if it does, the electrical resistance increases. The known electrical current is applied on the measuring part (I_{meas}) and on the reference part (I_{ref}) while the voltage drops at the measuring part (U_{meas}) and at the reference part (U_{ref}) are recorded at different positions. Such 4-point electrical resistance measurement results in the electrical resistance values of the measuring part (R_{meas}) and of the reference part (R_{ref}). This method provides real-time monitoring of the corrosion depth in broad variety of environments, such as atmospheric, marine, pipeline (corrosion under insulation), concrete, soils, etc. [16–18].

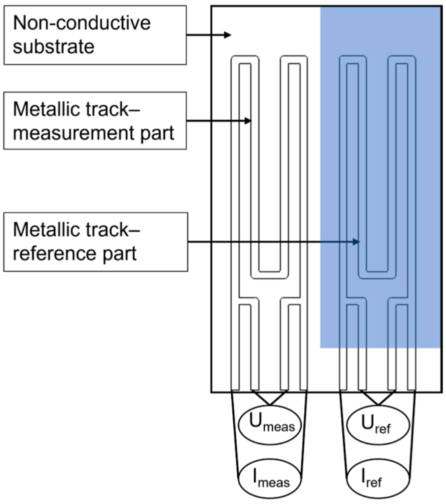

Figure 1. Schematic picture of a resistometric sensor.

The use of galvanized steel rebars in concrete raises questions in literature dealing with the mechanism of active-to-passive transfer, impact of pH and oxidizing power, morphology of corrosion products and bond strength with concrete, kinetics of corrosion and reduction reactions, especially within the first days of exposure, the overall consumption of zinc coating in fresh concrete, etc. The resistometric technique is a useful tool providing an answer to at least some of the questions related to corrosion kinetics and corrosion loss. Free corrosion potential monitoring at the same time provides information on the type of electrochemical reactions including the reduction one. The aim of our latest work was to demonstrate the possible applicability of the resistometric technique in the study of zinc corrosion in a concrete environment and to describe the kinetics of zinc corrosion during the transfer from activity to passivity in order to clarify the processes on zinc surfaces in concrete solutions. The applicability of resistometric sensors is well suited to these experiments due to the uniform corrosion of zinc under these conditions because localized corrosion detection presents a problem for the resistometric technique in terms of the measurement principle.

2. Materials and Methods

Resistometric sensors of the AirCorr type [17,19,20] were used to examine the corrosion depth (rate) of zinc in time. The purity of zinc used for the fabrication of sensors was 99.95% from GoodFellow Cambridge Ltd. (Huntingdon, UK). A schematic picture of the sensors used in these experiments is shown in Figure 1. The initial thickness of the zinc tracks was 50 µm. The zinc AirCorr type sensors were connected to the ACD-03 logger from MetriCorr (Rødovre, DK) which measured the electrical resistances of both the measurement and reference parts of the sensor every 10 min. The zinc corrosion depth was calculated using Formula (7), where h_0 stands for initial thickness of the zinc foil track, R_r and R_m stand for electrical resistance of the reference part and measurement part, respectively, and $R_{r,0}$ and $R_{m,0}$ stand for the initial resistances of both parts, as in [17]. The corrosion rate was calculated as a derivative of corrosion depth in time. Simultaneously, the free corrosion potential of the zinc track was recorded with respect to a saturated calomel electrode (SCE) by means of an Agilent 34970 datalogger, from Agilent Technologies (Santa Clara, CA, USA), also with a 10 min scanning interval.

$$\Delta h = h_0 \cdot \left(1 - \frac{R_r}{R_m} \cdot \frac{R_{m,0}}{R_{r,0}}\right) \tag{7}$$

Zinc sensors were pickled in 15 wt.% NaOH for 20 s and rinsed with tap water and then with distilled water right before each experiment. Then, the sensors were immersed in solution, simulating concrete conditions. Fresh concrete conditions were simulated by means of a saturated $Ca(OH)_2$ solution, the pH of which is approximately 12.5; carbonated concrete conditions were simulated by means of a solution composed of $NaHCO_3$ ($0.1\ mol \cdot L^{-1}$) and Na_2CO_3 ($5 \times 10^{-4}\ mol \cdot L^{-1}$) the pH of which was 8 [21]. Gradual chloride contamination was simulated by means of step-by-step additions of NaCl, resulting in different chloride content in the solutions ranging from 0.1 wt.% Cl^- to 0.9 wt.% Cl^-. The experimental setup is shown in Figure 2. The cell for the experiments is shown in Figure 2a, it consisted of the sensor and the reference electrode for corrosion potential monitoring of the sensor. The volume of all solutions was 400 mL. All experiments were conducted at laboratory temperature in open cells to maintain contact with air. Carbonation of the solution was prevented by the presence of solid $Ca(OH)_2$ in the solution. In the part of the test where carbonation was intentionally simulated, this phenomenon occurs naturally for $Ca(OH)_2$ saturated solutions, due to the interaction with CO_2 present in the air.

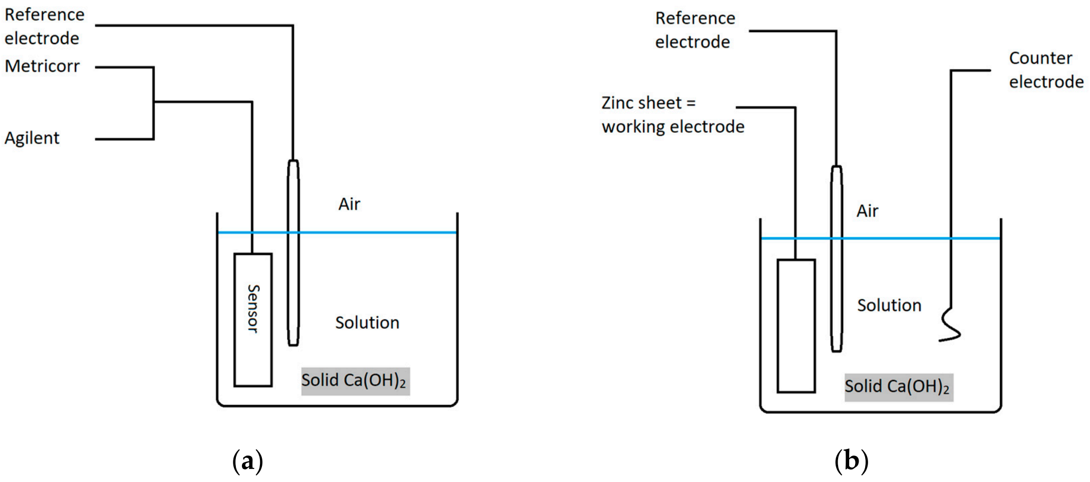

(**a**) (**b**)

Figure 2. Experimental procedure—scheme of electrochemical cell with resistometric sensor (**a**) and scheme of a common three-electrode cell for electrochemical impedance spectroscopy measurements (**b**).

The electrochemical impedance spectroscopy (EIS) measurement was conducted on a zinc sheet to confirm formation of a passive layer by other techniques. A zinc sheet of 99.5% purity was first ground to P600, pickled in 15 wt.% NaOH solution for 30 s, rinsed with water and finally immersed in the simulated concrete solution at laboratory temperature. The cell for EIS experiments is shown in Figure 2b, it consisted of a zinc sheet, a reference electrode and a counter electrode. The EIS measurements were conducted against a saturated calomel electrode (SCE, +0.241 V vs. SHE) and using a graphite counter electrode in 300 mL of a simulated concrete solution. EIS spectra were recorded at the frequency range from 100 kHz to 10 mHz with an amplitude of 5 mV. Six points were collected per decade. The EIS spectra were measured once every 2 h. The equivalent circuit for EIS evaluation is shown in Figure 3, it is the Randles circuit modified with two time constants and three resistors [22]. The changes in time of resistance of charge transfer (Rct) were evaluated to observe passivation of the zinc surface. The EIS was conducted with Gamry Interface 1010 from Gamry Instruments (Warminster, PA, USA).

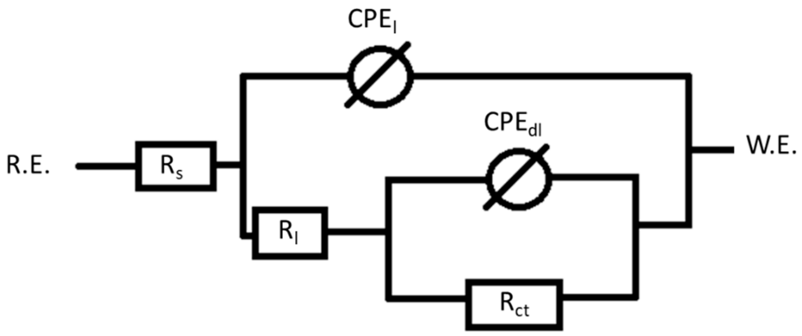

Figure 3. Equivalent circuit used for EIS measurements where R_s stands for solution resistance, R_{layer} and CPE_l—resistance and constant phase element for passive non-conductive layer, R_{ct} stands for resistance of charge transfer and CPE_{dl} is a constant phase element for a double layer.

3. Results and Discussion

3.1. Passivation of Zinc in a Simulated Concrete Solution

Zinc sensors were immersed in simulated concrete solution while the corrosion depth and free corrosion potential of zinc sensors were monitored. The behaviour of zinc sensors in a simulated fresh concrete solution (saturated $Ca(OH)_2$) remained very similar in all

8 experiments; at the beginning the zinc corroded actively and uniform corrosion of zinc occurred, after a certain time it became passive. The corrosion rate lowered, and the free potential changed rapidly, indicating the spontaneous transfer from an active to passive state. The time to the passivation in the simulated fresh concrete solution ranged from 6 to 30 h for the experiments.

The rapid change of the free corrosion potential and the corresponding change of zinc corrosion rate in a simulated fresh concrete solution is presented in Figure 4. The blue line represents the corrosion depth recorded by a resistometric sensor, and the orange line represents the free corrosion potential of an ER zinc probe with respect to SCE. The slope of the linear sections of the corrosion depth–time curve corresponds to the zinc corrosion rate in those particular sections. In this particular case (Figure 4), zinc became passive after 7 h of immersion in a simulated concrete solution. The rise of corrosion losses reached a plateau and at the same time the potential changed from −1400 mV/SCE to less negative values (−550 mV/SCE). Since the zinc became passive, the potential values stabilized at approx. −800 mV/SCE, which is in good agreement with a passive state potential according to the literature [10]. During active corrosion the potential of zinc was in the range where the hydrogen is thermodynamically stable instead of the water (dashed line in Figure 4 indicates the hydrogen/water equilibrium potential for pH 12.5), and hydrogen gas formation occurred. The zinc resistometric sensor when in passive state showed much slower corrosion consumption, with a corresponding corrosion rate about 40 times lower than during active corrosion. The process of active-to-passive transfer itself is rapid, the potential of zinc increased to a passive level within 1 measurement interval e.g., 10 min, but before passivation, 0.9 µm of zinc thickness got lost which means that within 7 h 1 cm^2 of zinc surface produced 0.24 cm^3 of hydrogen.

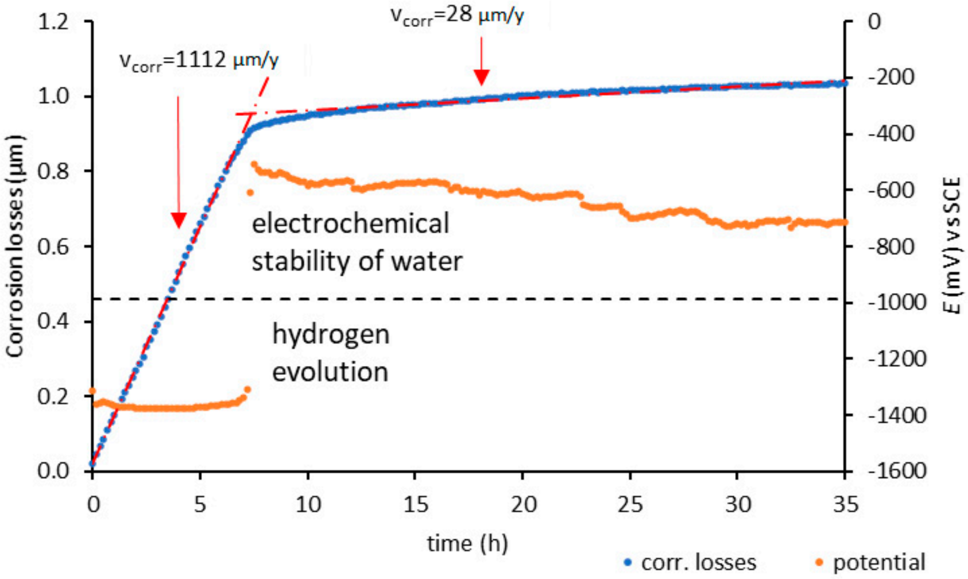

Figure 4. Record of corrosion losses and corrosion potential of zinc resistometric sensor in simulated concrete solution—process of passivation; black dashed black line indicates thermodynamic stability of water.

The corrosion behaviour of zinc in simulated concrete solution was studied also by means of EIS measurements. Two of the EIS are shown in Figure 5 in Nyquist plot spectra (the x-axis represents the real part of the transfer function and the y-axis represents the imaginary part of the function). The first spectrum (Figure 5a) shows the EIS spectrum of zinc during active corrosion, e.g., a few hours after immersion into the simulated fresh concrete solution. The spectrum in Figure 5b was obtained when a stable protective layer was already formed. The spectra were filtered using a Kramers–Kronig fit. The passivation is well observable in the charge transfer resistance, which represents the resistance of a material towards corrosion reactions. After approximately 17 h, the zinc sheet became passive and thus charge transfer resistance increased significantly, as Figure 6 shows. This means that the corrosion rate of zinc slowed down in agreement with the results given by the resistometric sensors during the passivation process (Figure 4).

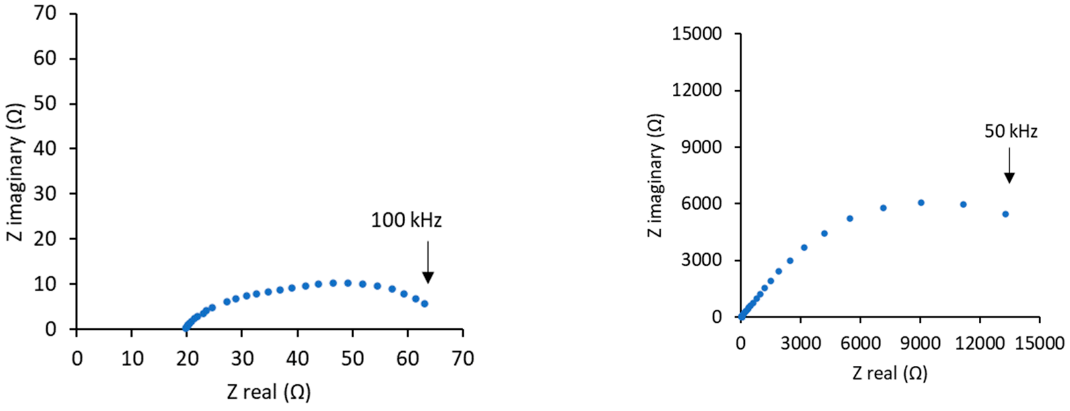

(**a**) (**b**)

Figure 5. EIS spectra of zinc sheet. After 2 h in a simulated concrete solution—active corrosion of zinc (**a**); after 24 h in a simulated concrete solution—passivity of zinc (**b**).

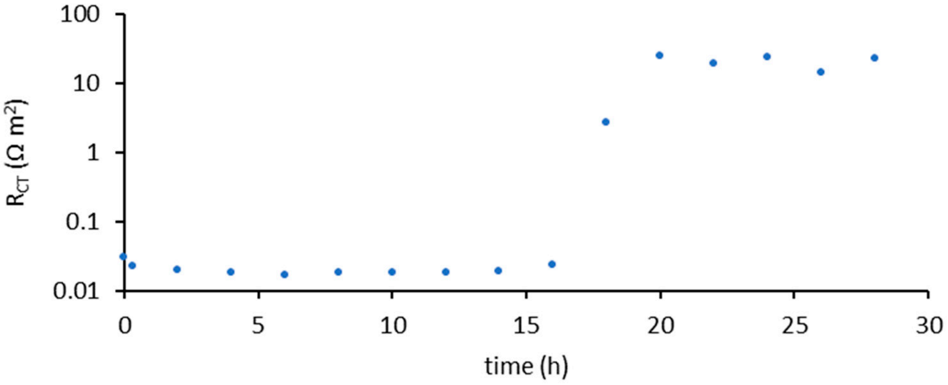

Figure 6. EIS results—resistance of charge transfer of zinc sheet in a simulated concrete solution.

The fact that the zinc is able to passivate in a simulated concrete solution is in agreement with the literature which supports galvanized steel application in concrete.

3.2. Behaviour of Passive Zinc in a Simulated Carbonated Concrete Solution

Zinc sensors were first immersed in a simulated fresh concrete solution (saturated $Ca(OH)_2$), and after 48 h the solution was replaced with simulated carbonated concrete solution (0.1 $mol \cdot L^{-1}$ $NaHCO_3$; 5×10^{-4} $mol \cdot L^{-1}$ Na_2CO_3). The corrosion loss and corrosion potential record in time are shown in Figure 7. Immersion of passive zinc into simulated carbonated solution resulted in corrosion activation of the zinc sensor for 5 h. After that, the zinc regained passivity based on a protective layer of a different composition. Most likely, the calcium hydroxyzincate-based protective layer changed into hydrozincite $Zn_5(CO_3)_2(OH)_6$ and calcite ($CaCO_3$), according to literature [7]. The new layer was protective as well, as can be seen in the low final corrosion rate of zinc in the simulated carbonated concrete solution. The time difference (>1 min) between the immersion into the simulated carbonate concrete solution (a vertical line at the 46th hour) and the initiation of rapid corrosion (at the 47th hour) corresponds to gradual depassivation. Within this period, a part of the surface is still protected by the calcium hydroxyzincate, but another part of the surface was already immediately activated, as proved by the immediate drop in free corrosion potential. Complete reconstruction of the protective layer, newly based on hydrozincite, was finished after 6 h in a simulated carbonated concrete solution, as the corrosion rate decreased and the free corrosion potential was re-established on a similar level to the previous solution. The ability of zinc to passivate in carbonated concrete leads to an extension of the service life of concrete structures.

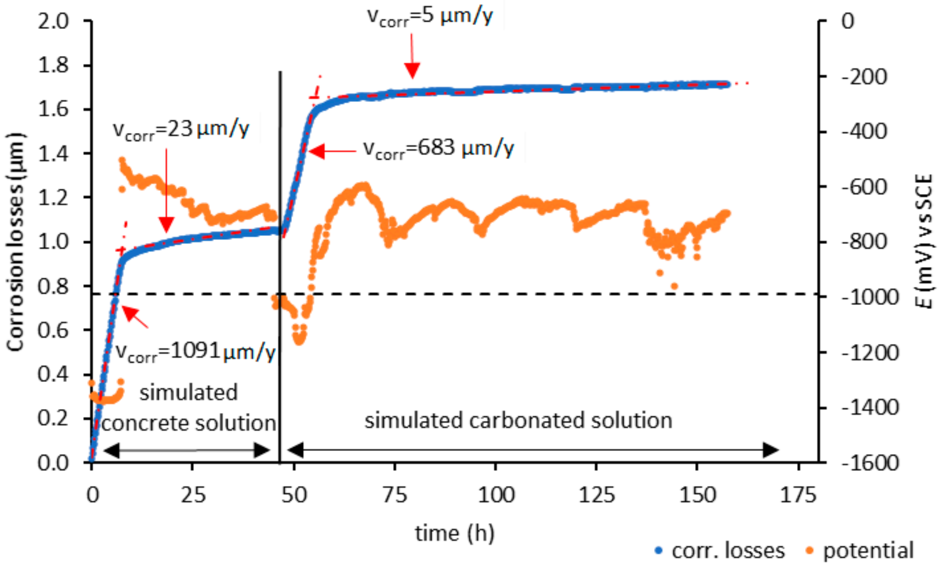

Figure 7. Record of corrosion losses and corrosion potential of a zinc sensor immersed in simulated concrete solution (until 48 h) and then in a simulated carbonated solution; the black dashed line represents the potential of thermodynamic stability of water; corrosion rates in µm per year are shown as v_{corr}.

3.3. Behaviour of Passive Zinc in Simulated Fresh Concrete Solution with Chlorides

First, the zinc resistometric sensor was immersed in the simulated fresh concrete solution. In this particular case, the passivation appeared after 12.5 h. Then, 12 h after the passivation of the sensor (24.5 h after immersion), a first dose of chlorides (0.3 wt.%) was dissolved in the solution. Subsequent doses increased the chloride content gradually up to the final chloride concentration of 0.9 wt.%. The graph of corrosion loss and free corrosion potential of the zinc sensor is plotted in Figure 8. The protective layer did not fail and the corrosion rate remained relatively low even up to the maximum chloride content, a chloride concentration of 0.9 wt.%. After each addition of chloride into the solution, the passive film became unstable and the corrosion potential dropped down temporarily, whereas the corrosion rate remained unaffected. The passive film instability could be interpreted as a transition of calcium hydroxyzincate into different corrosion products, due to the adding of chloride ions into the environment. According to the literature [12], simonkolleite ($Zn_5(OH)_8Cl_2 \cdot H_2O$) and zincite (ZnO) is formed on galvanized steel in the presence of chlorides. It is possible that the drops of free corrosion potential at 0.3 and 0.5 wt.% of chlorides and the final stabilization at 0.7 and 0.9 wt.% correspond to reconstruction of the protective layer at the zinc surface from calcium hydroxyzincate to simonkolleite, which would protect the zinc coating against rapid corrosion until the content of chlorides exceeds critical breakdown level.

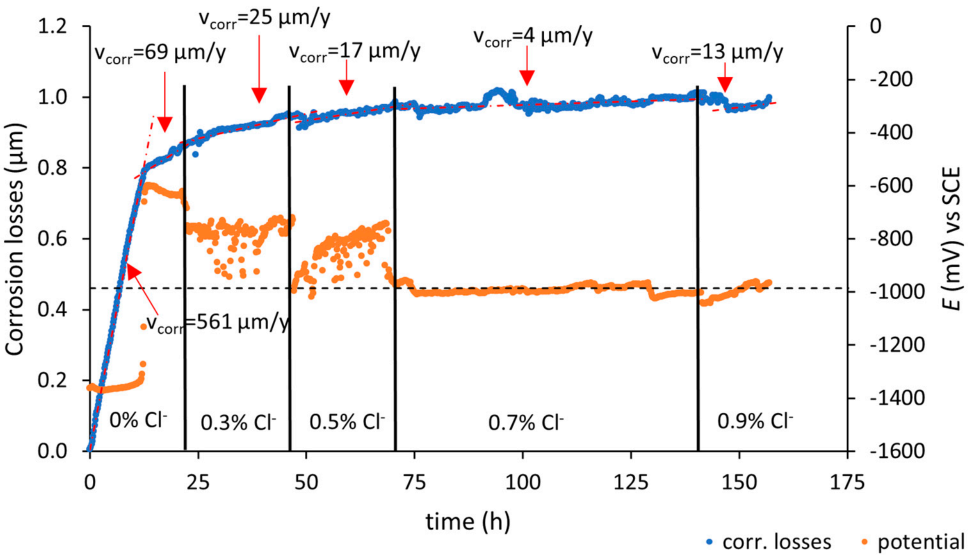

Figure 8. Record of corrosion losses and free potential of the zinc sensor in a simulated concrete solution with increasing amounts of chlorides; the black dashed line represents a potential of thermodynamic stability of water; corrosion rates in µm per year are shown as v_{corr}.

4. Conclusions

The corrosion rate measurement by means of zinc resistometric sensors confirmed that zinc is able to passivate under simulated fresh concrete conditions and even under simulated carbonated concrete conditions. Within 6–30 h, the zinc was able to become passive in a simulated fresh concrete solution (saturated $Ca(OH)_2$) due to a protective calcium hydroxyzincate (CHZ) layer. The corrosion potential of zinc before passivation falls in the potential area, in which the hydrogen is thermodynamically stable. Therefore, the zinc corrodes actively and the hydrogen is being produced until the stable passive layer is formed. The zinc corrosion rate was reduced by almost 40 times during the active to passive transition.

In the simulated carbonated concrete solution, the zinc loses its passivity and corrodes actively. Nevertheless, the zinc is able to regain passivity after a few hours. The composition of the protective layer is then different, probably based on hydrozincite. Such a protective layer seems to be less stable than the calcium hydroxyzincate-based layer, considering the fluctuations of the corrosion potential. These fluctuations point to a lower stability and the presence of local disruptions of the passive layer. The corrosion rate during this stage is still much lower than during active corrosion.

The presence of chlorides is a general problem for concrete reinforcement. Due to the increased aggressivity of the environment, the steel rebars undergo corrosion which leads to structural failure. Zinc in the environment of the simulated fresh concrete solution polluted with chloride anions remains passive. The corrosion rate remained very low (tenths of micrometres per year), like previous passive conditions, and the corrosion potential is moving towards a more negative value as the chloride content is higher. The shift of corrosion potential towards a more negative value points to a formation of different corrosion products based on $Zn_5(OH)_8Cl_2 \cdot H_2O$ and ZnO. High resolution zinc resistometric sensors didn't record any significant increase of corrosion rate within the tested range (0.0–0.9 wt.% Cl^-).

Author Contributions: Conceptualization, M.R. and M.K.; validation, M.K. and P.F.; writing—original draft preparation, M.R.; writing—review and editing, M.K., P.F. and T.B.; supervision, T.B.; project administration, M.R.; All authors have read and agreed to the published version of the manuscript.

Funding: This research was funded by the Czech Science Foundation, project number 21-11965S.

Data Availability Statement: The original contributions presented in this study are included in the article material. Further inquiries can be directed to the corresponding author. The complete set of data will be publicly available in the corresponding author's study.

Acknowledgments: The authors acknowledge financial support of the study program Erasmus+, which enabled cooperation between the University of Chemistry and Technology in Prague and Marche Polytechnic University.

Conflicts of Interest: The authors declare no conflicts of interest. The funders had no role in the design of the study; in the collection, analyses, or interpretation of data; in the writing of the manuscript; or in the decision to publish the results.

Abbreviations

The following abbreviations are used in this manuscript:

CHZ	Calcium hydroxyzincate
EIS	Electrochemical impedance spectroscopy
ER probe	Electrical resistance probe
SCE	Saturated calomel electrode

References

1. Hu, J.Y.; Zhang, S.S.; Chen, E.; Li, W.G. A review on corrosion detection and protection of existing reinforced concrete (RC) structures. *Constr. Build. Mater.* **2022**, *325*, 126718. [CrossRef]
2. Xu, Y.; Li, K.; Liu, L.; Yang, L.; Wang, X.; Huang, Y. Experimental Study on Rebar Corrosion Using the Galvanic Sensor Combined with the Electronic Resistance Technique. *Sensors* **2016**, *16*, 1451. [CrossRef] [PubMed]
3. Darwin, D.; O'Reilly, M.; Browning, J.; Locke, C.E.; Virmani, Y.P.; Ji, J.; Gong, L.; Guo, G.; Draper, J.; Xing, L. Multiple corrosion-protection systems for reinforced-concrete bridge components: Laboratory tests. *J. Mater. Civ. Eng.* **2014**, *26*, 04014085. [CrossRef]
4. Bellezze, T.; Mobili, A.; Tittarelli, F. Durability benefits of galvanized steel in reinforced concrete under different exposure conditions. In Proceedings of the CACRCS Workshop on Capacity Assessment of Corroded Reinforced Concrete Structures, Virtual, Online, 12–15 September 2021; pp. 45–48.
5. Yeomans, S.R. Galvanized steel reinforcement. In *Corrosion of Steel in Concrete Structures*; Woodhead Publishing: Cambridge, UK, 2016; pp. 111–129.
6. Maeda, M.; Li, X.; Ooi, A.; Tada, E.; Nishikata, A. Passivation Mechanism of Galvanized Steel Rebar in Fresh Concrete. *ISIJ Int.* **2020**, *60*, 337–345. [CrossRef]
7. Roventi, G.; Bellezze, T.; Barbaresi, E.; Fratesi, R. Effect of carbonation process on the passivating products of zinc in $Ca(OH)_2$ saturated solution. *Mater. Corros.* **2013**, *64*, 1007–1014. [CrossRef]
8. Tan, Z.Q.; Hansson, C.M. Effect of surface condition on the initial corrosion of galvanized reinforcing steel embedded in concrete. *Corros. Sci.* **2008**, *50*, 2512–2522. [CrossRef]
9. da Fonsêca, B.; Meira, G.R. Accelerated chloride-induced corrosion of hot-dipped galvanized reinforcements and its influence on bond strength to concrete. *Constr. Build. Mater.* **2024**, *426*, 136123. [CrossRef]
10. Tittarelli, F.; Bellezze, T. Investigation of the major reduction reaction occurring during the passivation of galvanized steel rebars. *Corros. Sci.* **2010**, *52*, 978–983. [CrossRef]
11. Darwin, D.; Browning, J.; O'Reilly, M.; Xing, L. Critical Chloride Corrosion Threshold of Galvanized Reinforcing Bars. *ACI Mater. J.* **2009**, *106*, 176–183.
12. Belaïd, F.A.; Francois, R.G. Corrosion products of galvanized rebars embedded in chloride-contaminated concrete. *Corrosion* **2000**, *56*, 5. [CrossRef]
13. Pernicova, R.; Dobias, D.; Pokorny, P. Problems Connected with use of Hot-dip Galvanized Reinforcement in Concrete Elements. *Procedia Eng.* **2017**, *172*, 859–866. [CrossRef]
14. Pokorný, P.; Kostelecka, M.; Prodanovic, N.; Sýkora, M. Effect of calcium hydroxyzincate on bond strength of hot-dip galvanized plain bars with normal strength concrete. *Cem. Concr. Compos.* **2022**, *130*, 104540. [CrossRef]

15. Pokorny, P.; Kouřil, M.; Kučera, V. Kinetics of Zinc Corrosion in Concrete as a Function of Water and Oxygen Availability. *Materials* **2019**, *12*, 2786. [CrossRef] [PubMed]
16. Reiser, M.; Sihlovec, F.; Beaudouin-Goujon, L.; Kouřil, M. Corrosive synergic effects of acetic acid and atmospheric pollutants on lead and zinc. *Koroze A Ochr. Mater.* **2022**, *66*, 113–125. [CrossRef]
17. Kouril, M.; Prosek, T.; Scheffel, B.; Dubois, F. High sensitivity electrical resistance sensors for indoor corrosion monitoring. *Corros. Eng. Sci. Technol.* **2013**, *48*, 282–287. [CrossRef]
18. Popova, K.; Prošek, T.; Šefl, V.; Šedivý, M.; Kouřil, M.; Reiser, M. Application of flexible resistometric sensors for real-time corrosion monitoring under insulation. *Mater. Corros.* **2024**, *75*, 625–635. [CrossRef]
19. Kouril, M.; Boháčková, T.; Strachotová, K.C.; Švadlena, J.; Prošek, T.; Kreislová, K.; Fialová, P. Lead Corrosion and Corrosivity Classification in Archives, Museums, and Churches. *Materials* **2022**, *15*, 639. [CrossRef] [PubMed]
20. Diler, E.; Peltier, F.; Becker, J.; Thierry, D. Real-time corrosion monitoring of aluminium alloys under chloride-contaminated atmospheric conditions. *Mater. Corros.* **2021**, *72*, 1377–1387. [CrossRef]
21. Criado, M.; Sobrados, I.; Bastidas, J.M.; Sanz, J. Steel corrosion in simulated carbonated concrete pore solution its protection using sol–gel coatings. *Prog. Org. Coat.* **2015**, *88*, 228–236. [CrossRef]
22. Christodoulou, C.; Goodier, C.I.; Austin, S.A.; Webb, J.; Glass, G. On-site transient analysis for the corrosion assessment of reinforced concrete. *Corros. Sci.* **2012**, *62*, 176–183. [CrossRef]